Theoretical Notes
Note 227

DNA 3411T

LOW FLUENCE CALCULATION OF PHOTOELECTRON FLUX DENSITIES OUTSIDE AN EMITTING SPHERE

TN227

Roger Stettner
Mission Research Corporation
735 State Street
Santa Barbara, California 93101

~~13 December~~ Jan 1974 1974

Topical Report

CONTRACT Nos. DNA 001-74-C-0032
DNA 001-73-C-0118

THIS WORK SPONSORED BY THE DEFENSE NUCLEAR AGENCY
UNDER SUBTASK R99QAXEB089-45.

Prepared for
Director
DEFENSE NUCLEAR AGENCY
Washington, D. C. 20305

TABLE OF CONTENTS

LIST OF ILLUSTRATIONS

SECTION 1

INTRODUCTION

In order to calculate the currents produced on the surface of a metal by an incident plane X-ray pulse, in the low-fluence limit, it is first necessary to incorporate a spatial source current in Maxwell's equations. In the low-fluence limit, for X rays not exceeding 100 kev (10^5 electron volts), the fields produced by backscattered electrons leaving the metal do not greatly influence their motion. Given the energy and angular distribution of electrons at the emitting surface one can construct a source current from the straight line motion of the electrons. This source allows an accurate solution of Maxwell's equation and hence also of the surface currents on the metal. The main purpose of this report is to discuss how such a source is constructed for a sphere where the electrons leave the surface according to a $\cos\alpha$ distribution; α is the angle made by an electron with the normal to the surface. Particular attention is paid to the position of the X-ray wavefront as it crosses the sphere since the initial rise of the electron flux with time may have an important influence on the amplitude of the resonant electromagnetic spherical modes stimulated. The position of the X-ray wavefront is also important for X-ray pulses whose duration is comparable to the time it takes light to cross the sphere.

Section 2 discusses the theoretical background and equations. Section 3 particularizes the discussion to a spherical surface emitting electrons with a $\cos\alpha$ distribution. Section 4 describes the numerical considerations incorporated in the computer code CUR2 which integrates the flux equations of Section 3. Section 5 discusses the results of the numerical calculation.

SECTION 2

THEORETICAL BACKGROUND

In this section an expression for the flux (number) density, J, of electrons outside a convex surface emitting photoelectrons will be derived. The current density is J multiplied by the charge of an electron. The emission results from a time varying plane-wave X ray crossing the surface. If the surface is a sphere, then, at most, half the sphere is emitting simultaneously.

Denoting the number of electrons emitted from a unit area of the surface, in the energy range dE and in the solid angle $d\Omega$ by

$$f(E, \alpha, t)d\Omega dE ,$$

where α is the angle made by the electron with the normal to the surface (reference can be made to Figure 1 which shows the situation for a sphere) then the number of electrons per unit area reaching a field point $\vec{r}$, from the surface element ds, in the direction $\vec{r} - \vec{r}_s$ is

$$\delta\vec{J}(\vec{r}, t) = \frac{\vec{r} - \vec{r}_s}{|\vec{r} - \vec{r}_s|^3} \int_{EMIN}^{EMAX} f\left(E, \alpha, t - \frac{|\vec{r} - \vec{r}_s|}{v}\right) dsdE, \quad (1)$$

where v is the speed of the particle and is given by the relativistic formula

$$v = \left(\frac{2E}{M_0}\right)\left[1 + \frac{E}{2M_0c^2}\right]^{1/2}\left[1 + \frac{E}{M_0c^2}\right]^{-1}, \quad (2)$$

where M_0 is the rest mass of the electron and c is the velocity of light. The retarded time

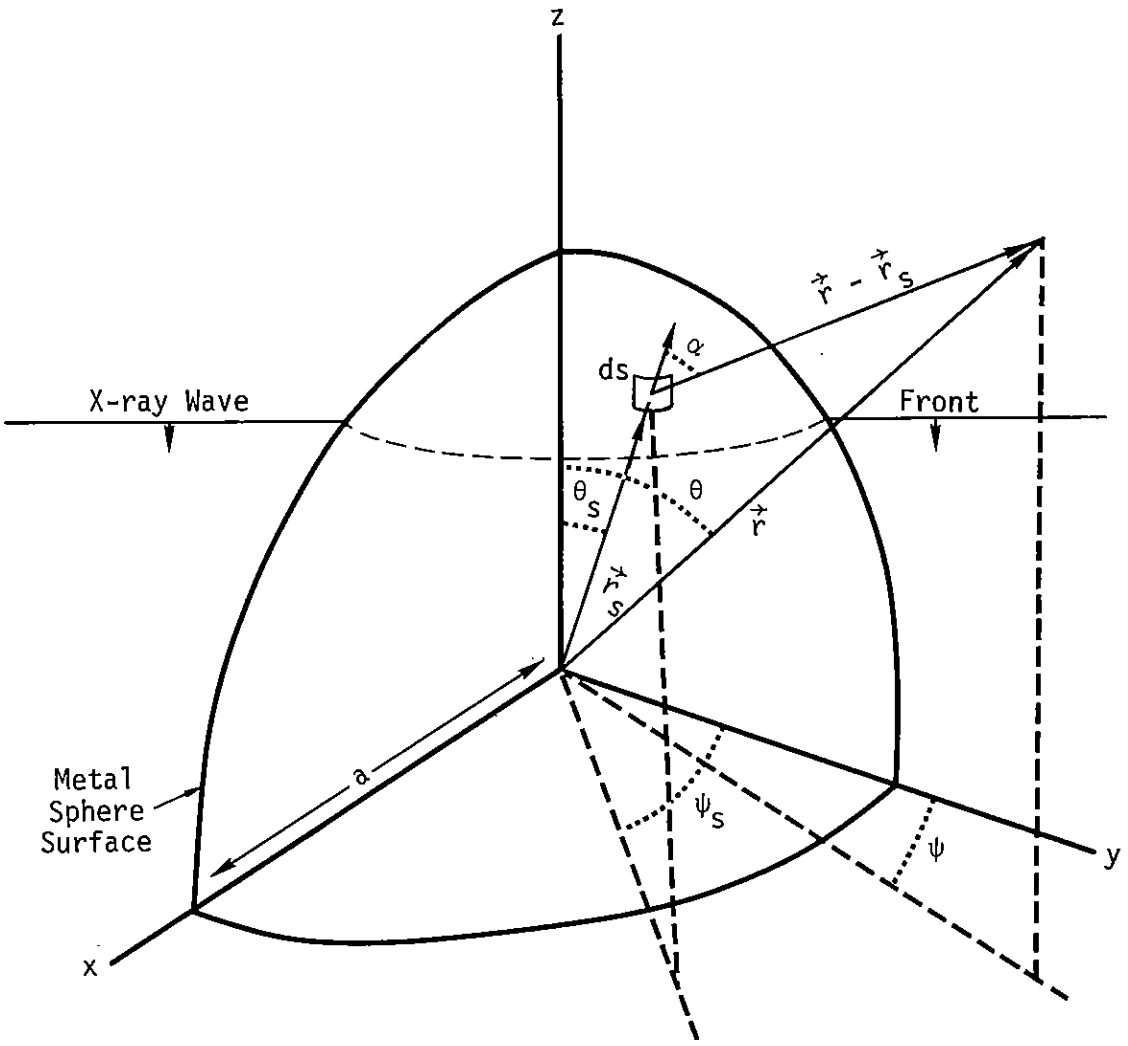

Figure 1. One-eighth of sphere.

$$t_R = t - \frac{|\vec{r} - \vec{r}_s|}{v} , \qquad (3)$$

(a subscript "s" refers to a variable on the emitting surface) occurs in Equation 1 because the particles arriving at the point $\vec{r}$ in time t were emitted at the earlier time t_R. The $(\vec{r} - \vec{r}_s)/|\vec{r} - \vec{r}_s|^3$ factor in Equation 1 expresses the inverse square dependence of the flux on the distance from a point emitter. The limit EMIN on the energy integral arises from the fact that not all electrons will be able to arrive at $\vec{r}$ at time t. If time is counted at the moment the X-ray wavefront arrives at ds then EMIN can be found by first finding the v at which $t_R = 0$ in Equation 3 and then substituting the result in Equation 2. In general, it is not quite so simple to find EMIN since the transit time of the wave across the surface must be considered. EMAX is in the maximum electron energy which equals the maximum X-ray photon energy.

If Equation 1 is integrated over the whole emitting surface, the total flux of electrons, $\vec{J}$, is

$$\vec{J}(\vec{r}, t) = \int_{s(t_R)} \left[\frac{(\vec{r} - \vec{r}_s)}{|\vec{r} - \vec{r}_s|^3} \int_{EMIN}^{EMAX} f(E, \alpha, t_R) dE \right] ds . \qquad (4)$$

The domain of integration in Equation 4 varies as the wavefront passes over the surface; the symbol $s(t_R)$ expresses that fact. If the time required by light to cross the object is small compared to the X-ray pulse length the domain of integration is, for the most part, the entire illuminated surface (for the case of a sphere the domain would be half of a sphere).

We now briefly mention the class of solutions of the Boltzman equation that Equation 4 is related to. The purpose of doing so is to show the possibility of calculating average properties of the

electron gas leaving the surface—such as its pressure. The collisionless force-free Boltzman equation is

$$\frac{\partial}{\partial t} f(\vec{r}, \vec{v}, t) + \vec{v} \cdot \vec{\nabla} f(\vec{r}, \vec{v}, t) = 0 \ . \tag{5}$$

Due to the straight line motion, for any velocity $\vec{v}$ in velocity space there exists an $\vec{r}_s$ such that

$$\vec{v} = v \frac{(\vec{r} - \vec{r}_s)}{|\vec{r} - \vec{r}_s|} \ . \tag{6}$$

Since the energy, E, is a constant of motion, a solution to Equation 5 is

$$f(\vec{r}, \vec{v}, t) = g(E, t_R) \ , \tag{7}$$

where

$$t_R = t - \frac{|r - r_s|}{v} \ . \tag{8}$$

The function g is determined from the boundary conditions at the surface s.

SECTION 3

THE SPHERICAL SURFACE

In this section we derive the form of expression (4) that is numerically integrated on a sphere. In the discussion that follows reference should be made to Figure 1 for the definition of the variables. A spherical coordinate system is chosen for the integration on the sphere and so we will eventually express the integrand in Equation 4 in terms of these variables. Since the problem is axially symmetric, the resulting fluxes, $\vec{J}$, will be independent of ψ (but the integrand is dependent on the surface coordinate ψ_s) and could be calculated in any plane containing the z axis. For convenience we take the plane $\psi = 0$. Due to the symmetry, $\vec{J}$ will have components only in the $\hat{r}$ and $\hat{\theta}$ directions, J_r and J_θ respectively. The integrand in Equation 4 is singular at the surface ($\vec{r} = \vec{r}_s$) and so to avoid a large error in the numerical integration near the surface the integrand will be transformed, through two transformations, to a new set of variables. The flux near the surface is important for electromagnetic problems designed to calculate surface currents so the error in calculation should be small. Since it is intended that the electron flux be calculated at many points and at many different times the calculation time must be small. The transformation of variables satisfies these conditions.

We first rotate the coordinates about the x axis so that the new z axis points in the direction of the point at which we wish to evaluate the field, $\vec{r}$. All coordinates referred to the original

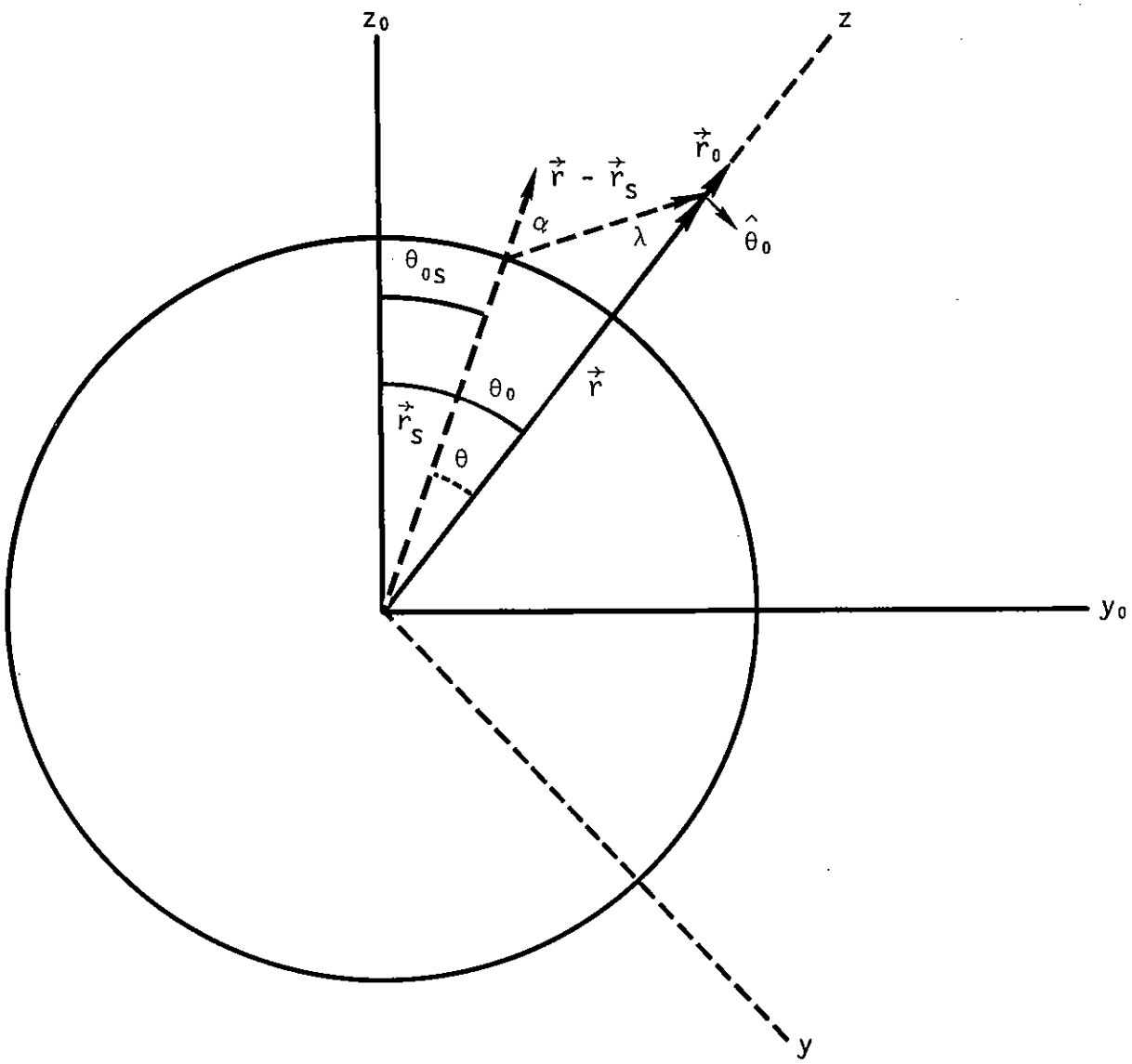

Figure 2. $\psi_0 = 0$ plane.

non-rotated frame of reference will, from this point on in the discussion, be subscripted with a "0." Coordinates referred to the new, rotated frame of reference will not be subscripted. The relation between the coordinates is depicted in Figure 2. In these new coordinates J_{r_0} is J_z and J_{θ_0} is J_y. The transformation simplifies the expression for $|\vec{r} - \vec{r}_s|$ in Equation 4 making it dependent on θ instead of θ_{0s} and ψ_{0s} but it has the disadvantage that the ψ integration is now dependent upon θ. As yet the singularity has not been removed.

Equation 4 will now be expressed in terms of the new coordinates. We assume

$$f(E, \alpha, t) = f(E, t) \frac{\cos\alpha}{\pi} , \tag{9}$$

where α is the angle between the normal to the surface and direction to the field point at ds. We have

$$\cos\alpha = \frac{r\cos\theta - a}{|\vec{r} - \vec{r}_s|} , \tag{10}$$

$$(\vec{r} - \vec{r}_s) \cdot \hat{k} = r - a\cos\theta , \tag{11}$$

$$(\vec{r} - \vec{r}_s) \cdot \hat{j} = - a\sin\theta , \tag{12}$$

$$|\vec{r} - \vec{r}_s|^2 = r^2 + a^2 - 2a\cos\theta , \tag{13}$$

where a is the radius of the sphere. Substituting Equations 9 through 13 into Equation 4, we find

$$J_z(\vec{r}, t) = \frac{1}{\pi}\int \frac{(r - a\cos\theta)(r\cos\theta - a)ds}{(r^2 + a^2 - 2a\cos\theta)^2} \int_{EMIN}^{EMAX} f(E, t_R)dE , \tag{14}$$

$$J_y(\vec{r}, t) = -\frac{1}{\pi}\int \frac{(a\sin\theta)(r\cos\theta - a)ds}{(r^2 + a^2 - 2a\cos\theta)^2} \int_{EMIN}^{EMAX} f(E, t_R)dE . \tag{15}$$

We make the second transformation to the new variable λ (see Figure 2):

$$\cos\lambda = \frac{r - a\cos\theta}{|\vec{r} - \vec{r}_s|} , \tag{16}$$

$$\sin\lambda = \frac{a\sin\theta}{|\vec{r} - \vec{r}_s|} , \tag{17}$$

$$d(\cos\lambda) = \frac{a^2(r\cos\theta - a)}{|\vec{r} - \vec{r}_s|^3} d(\cos\theta) . \tag{18}$$

Substituting Equations 16 through 18 into Equations 14 and 15 while using the fact that $ds = -a^2 d\cos\theta d\psi$ we find

$$J_z = -\frac{1}{\pi}\int d\cos\lambda\cos\lambda d\psi \int_{EMAX}^{EMIN} f(E, t_R)dE , \tag{19}$$

$$J_y = +\frac{1}{\pi}\int d\cos\lambda\sin\lambda d\psi \int_{EMAX}^{EMIN} f(E, t_R)dE . \tag{20}$$

Equations 19 and 20 give the J_{r_0} and J_{θ_0} fluxes, respectively, in the original coordinate system. They are the expressions that will be numerically integrated. The numerical calculation will be described in the next sections.

SECTION 4

NUMERICAL CALCULATION

In this section the numerical integration of Equations 19 and 20 will be described. The ψ integration depends on λ (or equivalently θ) since it takes the range from π to the intersection of the X-ray wavefront with the sphere (when the wavefront passes onto the negative z_0 axis the intersection is maintained at $z_0 = 0$); the ψ integration is also time dependent.

At a given field point $\vec{r}$ and at a time t the integration is begun by finding a λ range. The λ range is broken into N1 sections (N1 annular rings). For each of these N1 sections (or N1 + 1 λ values—these values are labeled by i) a maximum ψ range is found. The ψ range is then divided into N2 sections (or N2 + 1 ψ values—these values are labeled j). Thus the surface is divided into N1 × N2 sections for the purposes of integration. Integration then proceeds as follows: For a given i the energy integral is performed for each corresponding j. These integrals are then added by means of an integration algorithm to obtain the integration on the ψ variable. These i sums are then added to yield the integration on λ. The parts of this section to follow detail the latter procedures.

λ RANGE

Since the particles travel in straight lines, the maximum λ angle from which a particle can reach the field point, r, occurs when the particle is emitted from a point on the sphere with a velocity perpendicular to the radius at that point. That is, the maximum λ angle at $\vec{r}$ is defined when the

emitted particle's motion is tangent to the sphere. Hence from Figure 2

$$\lambda_{MAX} = \sin^{-1} a/r \ . \tag{21}$$

For most all values of t_R the sphere emits from λ_{MAX} to zero. When t_R is small however the wavefront may not yet have passed through the entire range $\lambda_{MAX} < \lambda < 0$. In such cases the ψ integration range will be found to be zero for those λ values which are not valid integration points. The integral will then be zero at the invalid points. The error made is small since the time required by light to cross the distance $a\Delta\theta$ ($\Delta\theta$ corresponds to a division of the λ range $\Delta\lambda$) is always small compared to pulse width.

ψ RANGE

If the duration of the X-ray pulse is long compared with the time it takes light to cross the sphere then, for the most part, after particles begin getting to $\vec{r}$, the whole half sphere is producing these particles. However, during the initial part of the electron flux pulse in space and especially for one resulting from an X ray of short duration the t_R position of the X-ray wavefront is not yet at the center of the sphere. The whole half sphere is therefore not yet producing particles which reach $\vec{r}$ at time t. In order to find that portion of the sphere which is producing particles we first find the minimum angle, ψ MIN,—the ψ integration is set up from π to ψ MIN—for which an electron with the maximum energy can just get to $\vec{r}$ at the time t.

In order to calculate ψ MIN we first calculate the time, TXF, necessary for the fastest electron—denote its velocity by v_x—to get to $\vec{r}$ from a given angle λ in the λ range.

$$TXF = \frac{\sqrt{r^2 + a^2 - 2a\cos\theta}}{v_x} , \tag{22}$$

where $\cos\theta$ is obtained from λ through Equation 16. The term in the numerator on the right-hand side of Equation 22 is just the distance from any point on a constant λ circle to $\vec{r}$. For an electron with speed v_x to get to $\vec{r}$ from all positions the wavefront has passed, on a constant λ circle, the wavefront can only have reached a position

$$z_0 = a - c(t - TXF) \ , \tag{23}$$

where $a \geq z_0 \geq 0$ and c is the speed of light. The ψ coordinate of the intersection of the plane at z_0 with the constant λ circle is

$$\cos \psi \text{ MIN} = \frac{\cos\theta\cos\theta_0 - z_0/a}{\sin\theta\sin\theta_0} \ , \tag{24}$$

where θ_0 is the angular coordinate of $\vec{r}$ in the original system of coordinates ($\psi_0 = 0$) and we require $\pi \geq \psi \text{ MIN} \geq 0$; if the right-hand side of Equation 24 is ≥ 1 for some θ then ψ MIN equals zero, if the right-hand side is ≤ -1 ψ MIN equals π (that is no electrons are emitted at this point).

INTEGRATION OVER THE ENERGY RANGE

When a decision is made upon a λ and ψ range for a given $\vec{r}$ and t the energy integration is performed for each of the (i, j) points. To find the lower limit of integration on the energy for a particular (i, j) point we decide the minimum speed an electron must have to get to $\vec{r}$ at t. For an electron with speed v coming from (i, j) the time t_R at which the distribution function must be evaluated involves both the time required for the electron to get to $\vec{r}$ from the surface-flight time—and the time required for the wavefront to get to (i, j). The formula

$$t_R = t - \frac{\sqrt{r^2+a^2- 2ar\cos\theta_i}}{v}$$

$$- a/c(1 + \cos\psi_j\sin\theta_0\sin\theta_i - \cos\theta_0\cos\theta_i) \ , \tag{25}$$

gives the value of t_R where the second term on the right-hand side gives the flight time and the third term is the time required for the wavefront to get to (i, j); θ_0 is the angular coordinate of $\vec{r}$ in the original coordinate system; ψ_j and θ_i are the coordinates of the emission point in the new spherical coordinate system. (The third term is found by finding the z_0 value for a plane intersecting the sphere at (i, j) and then finding how long it takes light to travel from $Z_0 = a$ to the intersection.) The smallest possible value of t_R is zero. Solving Equation 25 for v at $t_R = 0$ and substituting the result in Equation 2 yields EMIN.

The range EMIN $\leq$ E $\leq$ EMAX is then divided into sections and Equations 19 through 20 are integrated on E. When $f(E, t_R)$ is evaluated the value of t_R corresponding to each E is given by Equation 25.

Since an energy integration is performed for each (i, j) point the speed with which it is computed is crucial to the speed of the entire program. For the energy spectrum used in the calculation, a six point Gaussian algorithm[2] gave better than 1 percent error. The energy spectrum used has the form

$$f(E, t) \sim e^{-.1E}\sin^2(t\omega) \ , \tag{26}$$

(see Equation 33 for the exact form of Equation 26) where if τ is the time width of the pulse

$$\tau\omega = \pi \ . \tag{27}$$

The integral is first transformed so that it is amenable to high accuracy with few integration points by means of

$$q^2 = E \ , \tag{28}$$

q is the new integration variable. The new range of integration is then

$$d < q < b \ , \tag{29}$$

if

$$d = (EMIN)^{1/2}$$
$$b = (EMAX)^{1/2} . \qquad (30)$$

The integrand is further transformed so that the integration is symmetric about zero by means of

$$s = 1/2(b - d)q + 1/2(d + b) ; \qquad (31)$$

s is the new integration variable and has the range

$$-1 < s < 1 . \qquad (32)$$

A six point Gaussian quadrature is performed over the doubly transformed integrand.

INTEGRATION OVER THE ψ RANGE

After the energy integration is completed for each (i, j) point—call this number I_{ij}—the ψ integration can be done. I_{ij} depends on j (on ψ) only through the third term in Equation 25. When this term is small compared to the sum of the first two terms the ψ integration can be done analytically. (That is, under the right circumstances Equations 14 and 15 require just a two-dimensional numerical integration greatly reducing the running time of the computer code. See page 21.)

The integration algorithm used to integrate on the ψ variable is Simpson's rule[2]. In the actual computation and in the graphs presented in this report the ψ range was divided into 20 intervals to insure 1 percent accuracy.

INTEGRATION OVER THE λ RANGE

Integration over the λ range in Equations 14 and 15 is much the same as the ψ integration; a Simpson's rule algorithm is used. In actual calculations and in the graphs presented in this report, the λ range was divided into 20 intervals.

SECTION 5

NUMERICAL RESULTS

In this section we present numerical results which represent general characteristics of the electron flux outside the sphere. The results were obtained from running the computer code CUR2 (described in the last paragraph of this section) at various times and at various locations in space. The distribution chosen for data presentation in this report is

$$f(E, t) = \frac{18 \times 10^5}{\tau} e^{-.11E} \sin(t\pi/\tau) , \qquad (33)$$

where $\tau = 3 \times 10^{-8}$ sec. Equation 33 represents the backscattered distribution of electrons caused by X-rays with a blackbody energy spectrum striking an aluminum surface[3, 4, 5]. The sphere is taken to have a radius of 1 meter EMAX = 100 kev.

Figure 3 shows the particle current in the $\hat{r}_0$ direction, J_{r_0}, as a function of time (time is counted from when the X-ray front intersects the sphere) at $\theta_0 = 0$ for two radial coordinates, 2 and 4 meters respectively, when $5 < E < 100$ kev. The particle current in the $\hat{\theta}_0$ direction is zero at $\theta_0 = 0$. As the radial coordinate increases the electron flux increases in duration and decreases in amplitude. The increase in duration is due, for the most part, to the increasing time of flight of the slower electrons; the decrease in amplitude is due roughly to the $1/r^2$ spreading of the particles as they leave the sphere.

Figure 4 shows the electron flux at the same two radial coordinates and the same energy range but at $\theta_0 = \pi/2$. J_{θ_0} is a small

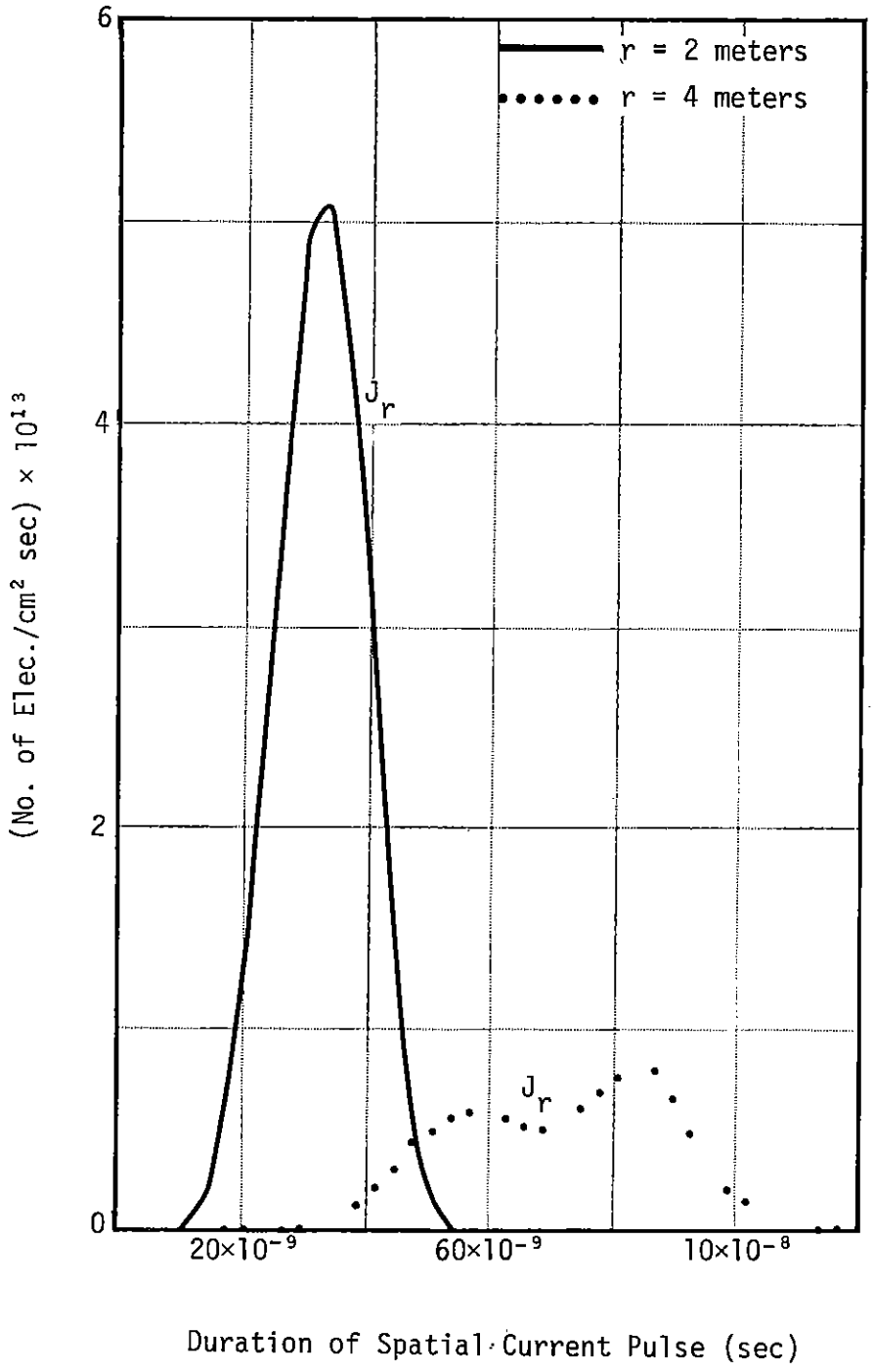

Figure 3. Electron flux vs. time $5 \leq E \leq 100$ kev, $\theta = 0$.

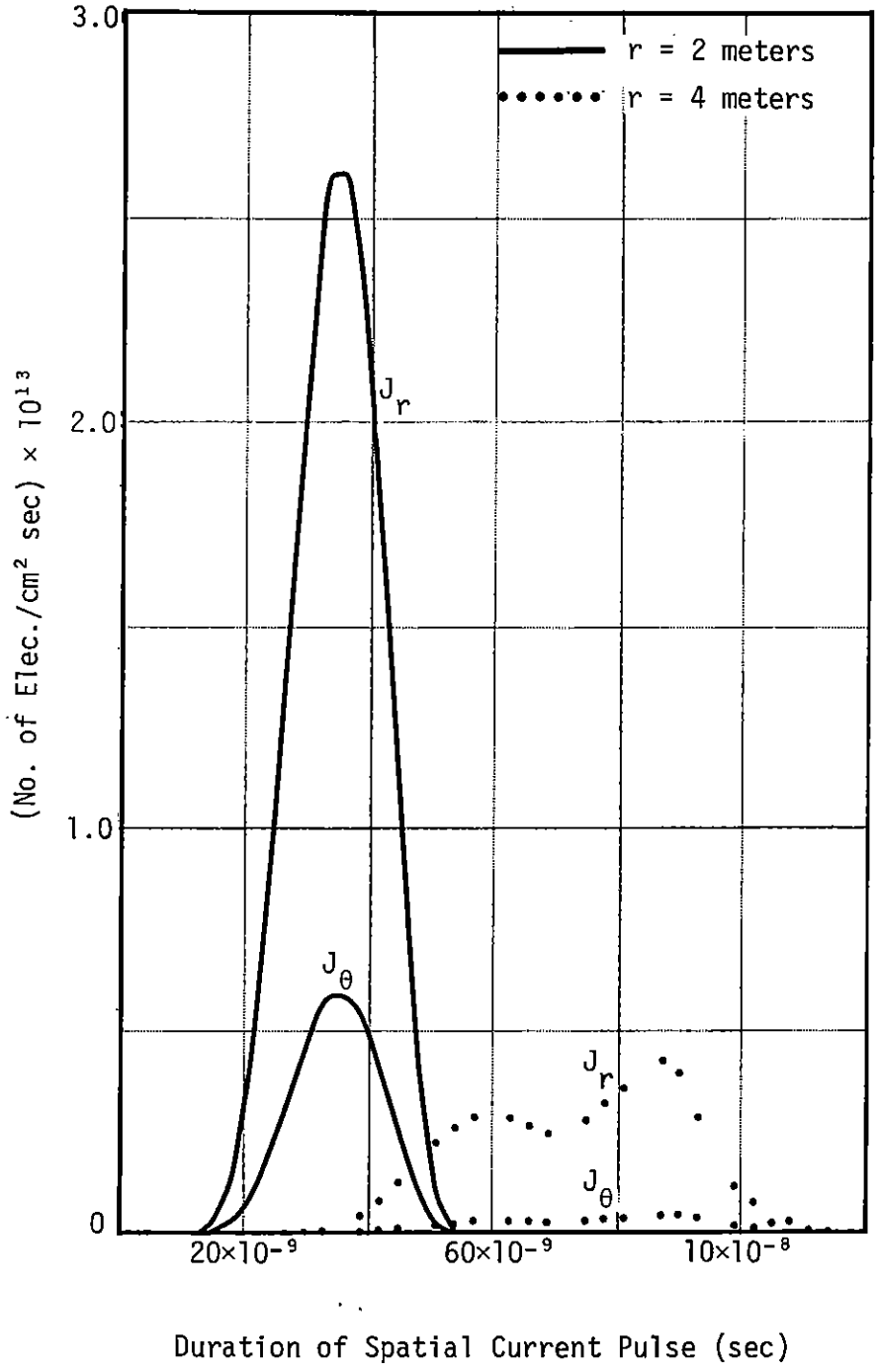

Figure 4. Electron flux vs. time $5 \leq E \leq 100$ kev, $\theta_0 = \pi/2$.

fraction of J_{r_0} in Figure 4 and also in general.

Figure 5 shows the angular variation of the two components of the electron flux at a radial coordinate of 2 meters and at a time equal to 2.4×10^{-8} seconds. The energy range is the same as the previous figure.

Figure 6 should be compared with Figure 3. Here slower electrons are added to the electron flux by decreasing the lower end of the energy range to zero. As expected, the duration of the electron flux is considerably broadened.

The running time for CUR2 for a given value of r_0, θ_0, t is .25 seconds on a CDC 7600. The running time is reduced by a factor of twenty when the integral is independent of ψ, as mentioned in Section 4 under Integration Over the ψ Range. Where CUR2 was used as a current source for Maxwell's equations a table was made for the currents at discrete times and positions. Linear interpolation was used to calculate the currents between the table points.

CUR2 will calculate the particle fluxes at any point in space from a sphere of arbitrary size if the emitted particle distribution at the surface is given. The code is set up to treat distributions of the functional form e^{-gE} where g is a constant and E is the particle energy; it could easily be adapted to distributions with other functional forms. The code will not treat emitting surfaces which are other than spherical however.

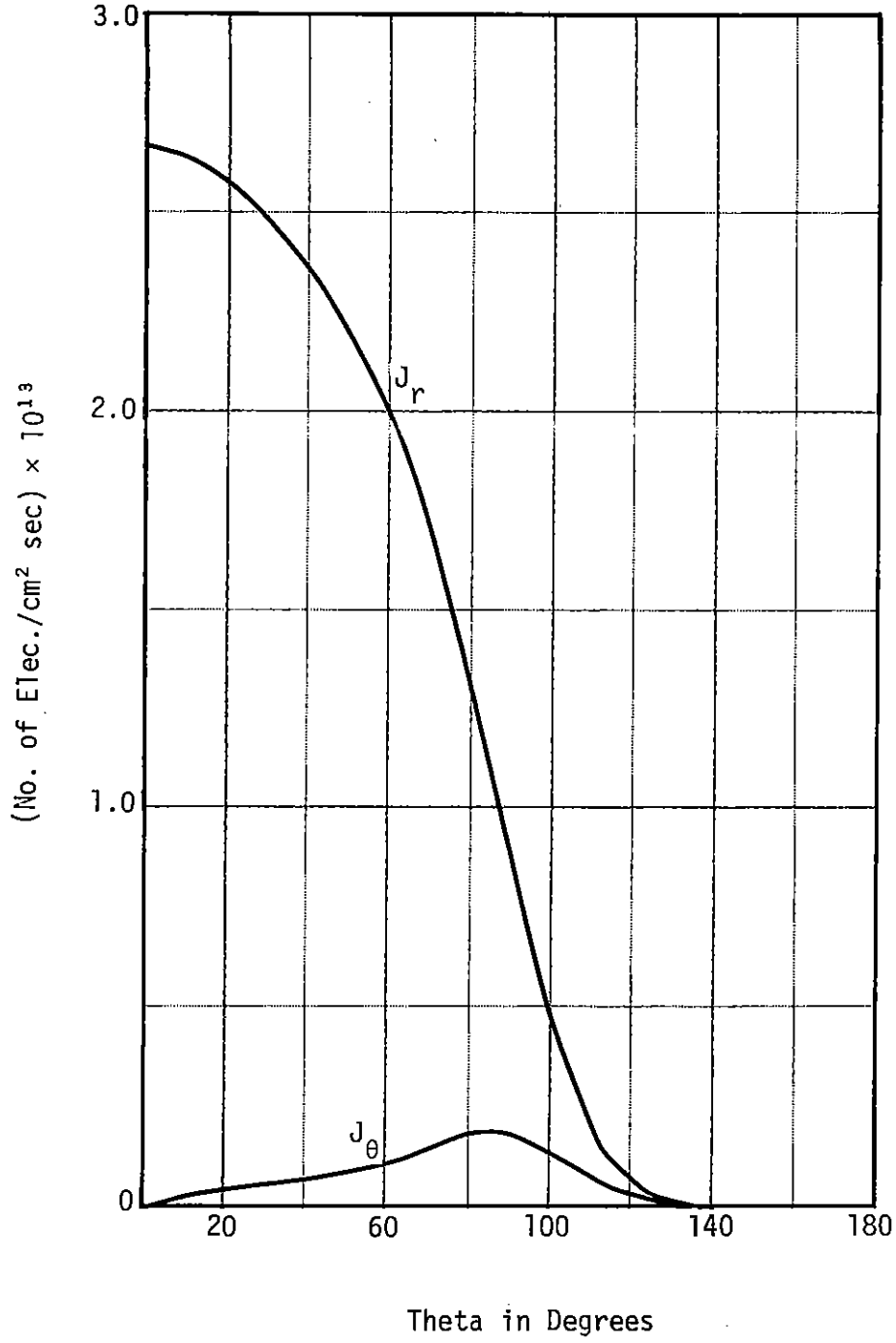

Figure 5. Electron flux vs. angle r = 2 meters, $t = 2.4 \times 10^{-8}$ sec, $5 < E < 100$ kev.

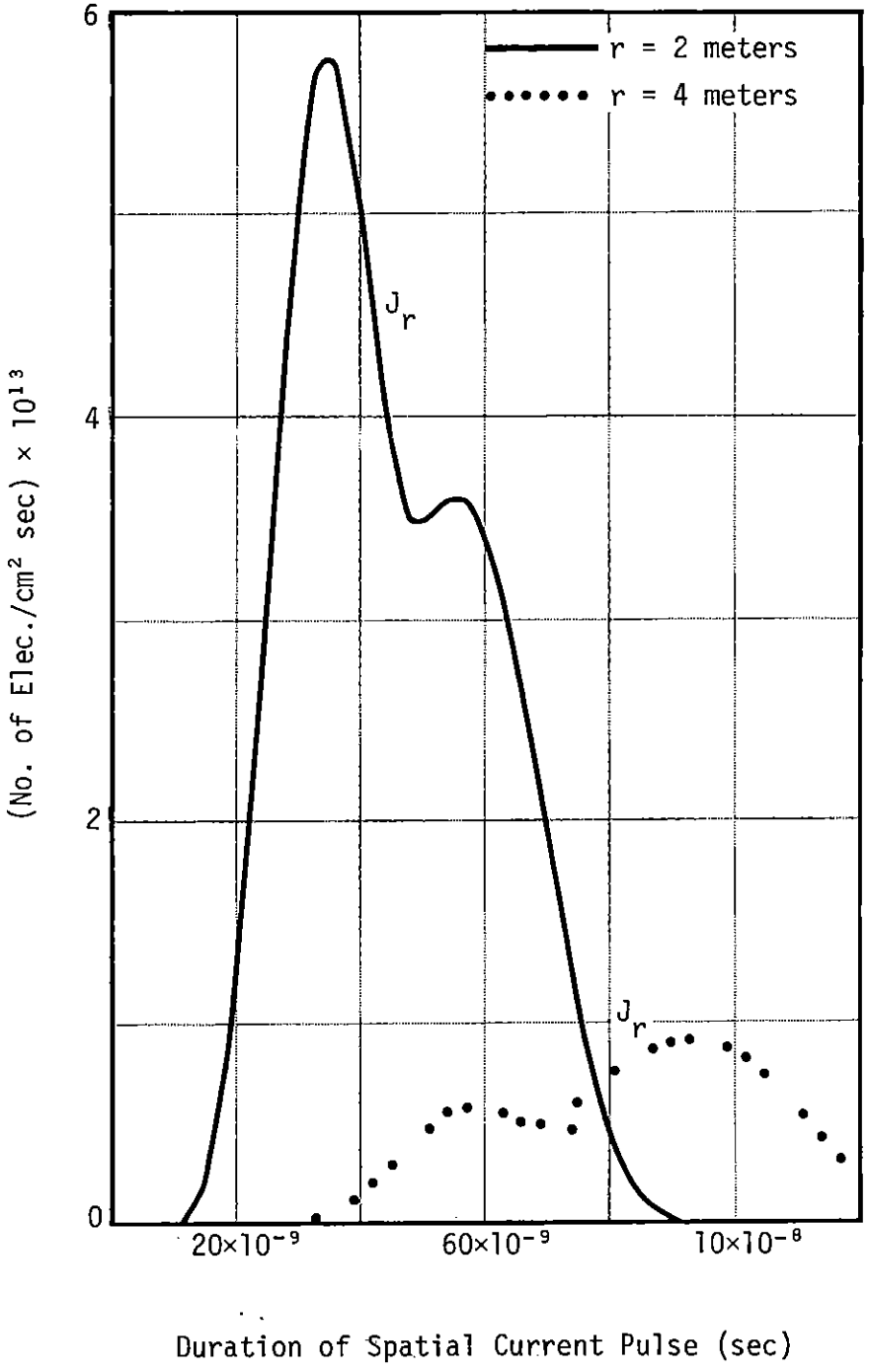

Figure 6. Electron flux vs. time $0 < E < 100$ kev, $\theta = 0$.

REFERENCES

1. Stettner, R., and D. F. Higgins, X-ray Induced Currents on the Surface of a Metalic Sphere, Mission Research Corporation, MRC-N-111, December 1973.

2. Conte, S. D., Elementary Numerical Analysis, McGraw-Hill, 1965.

3. Higgins, D. F., X-ray Induced Photoelectric Currents, Mission Research Corporation, MRC-R-81, June 1973.

4. Longmire, C. L., Tank Physics Memo 3, Mission Research Corporation, August 1972.

5. Longmire, C. L., Tank Physics Memo 6, Mission Research Corporation, September 1972.